Korean J. Chem. Eng., **28**(5), 1181-1187 (2011)
DOI: 10.1007/s11814-010-0481-3

Computational fluid dynamics modeling of high temperature air combustion in an heat recovery steam generator boiler

Abhas Khoshhal*, Masoud Rahimi*,†, Afshar Ghahramani*, and Ammar Abdulaziz Alsairafi**

*CFD Research Centre, Chemical Engineering Department, Razi University, Kermanshah, Iran
**Faculty of Mechanical Engineering, College of Engineering and Petroleum, Kuwait University, Kuwait
(*Received 19 August 2010 • accepted 15 November 2010*)

Abstract−This paper reports a numerical study on the possibility of using high temperature air combustion (HiTAC) technique in the heat recovery steam generator (HRSG) boiler of the Fajr Petrochemical Complex, Iran. For this purpose a theoretical fuel nozzle which operates in HiTAC mode of combustion has been installed and modeled using the computational fluid dynamics (CFD) technique. By aim of establishing an efficient heat transfer rate to the boiler's tubes, the proper nozzle location and an optimum mass flow rate of fuel have been found. The results show that by using this modification it is possible to increase the steam temperature up to 37 percent.

Key words: CFD, HiTAC, HRSG Boiler, Modeling, Heat Transfer

INTRODUCTION

Rapid industrialization and growth of human society has resulted in rapid utilization of earth's natural resources. The high temperature air combustion (HiTAC) technique, developed by Tanaka and Hasegawa [1], is one of the most promising combustion techniques which provides a solution for energy saving, energy efficiency and pollution control. The HiTAC technique is one of the most advanced techniques because of low levels of NOx formation and emissions [2-5]. In HiTAC technology a low oxygen concentration oxidizer at high temperatures is used for combustion. In conventional burners an increase in the temperature of preheated air increases the NOx emission levels. In the HiTAC combustion technique, the oxygen concentration in the combustion air is very low, and under this condition the thermal field in the combustion zone is quite uniform. The peak temperatures in the combustion zone are suppressed to result in very low NOx emission levels [6].

Although the technology of fuel combustion with highly preheated air has substantially improved over the last decade or so, limited work [7] has been undertaken by the fundamental combustion community to support the development.

In many industrial combustion systems the fuel jets emerge into a hot environment of oxidants and products [8]. Lille et al. [9] built an experimental facility to study fuel jets immersed into a cross-flowing high temperature air stream in order to enhance mixing and attain flameless conditions. In another study, Kim et al. [10] used the conditional moment closure (CMC) method to model turbulent jet diffusion flames into a hot and diluted surroundings with some success.

The numerical modeling of the combustion process in industrial boilers is a complicated calculation that involves modeling of turbulent flow, combustion and radiation. Due to progress in computer hardware and software and the consequent increase of the calculation speed, the computational fluid dynamics (CFD) modeling technique would be a powerful and effective tool for understanding the complex hydrodynamics in many industrial processes [11-14].

Using HiTAC combustion burner has recently found considerable attention as a promising system for industrial boilers and furnaces. Orsino et al. [15] assessed the abilities of existing combustion models to predict the characteristics of the HiTAC technology in a semi-industrial or industrial furnace. They reported that the available numerical models, for instance, the eddy-break-up model, eddy-dissipation concept model with chemical equilibrium, and a PDF/mixture fraction model with equilibrium, can correctly reproduce the characteristics of the high temperature air combustion. However, they believe that these models cannot describe the chemistry and temperature field in the fuel jet region.

In another research, a new boiler using high temperature preheated air was introduced by Kawai et al. [16]. The boiler was characterized by uniform heat flux field, augmentation of heat transfer, reduction of combustion noise level, suppression of NOx emission and compactness. On the other hand, the effects of using a diluted fuel in an industrial furnace under several cases of conventional combustion and the highly preheated and diluted air combustion (HPDAC) was numerically studied by Khazaei et al. [17]. They found a decrease in NOx pollutant formation in case of employing the HPDAC technique.

The heat recovery steam generator (HRSG) is a type of boiler which uses heat recovery of hot output gases from gas turbines for generating steam. The generated steam is turned into electrical power through the steam turbines in power plants. An analysis of some possibilities to increase the combined cycle plant efficiency to values higher than the 60% in this type of steam generators, without resorting to a new gas turbine technology, was investigated by Franco and Casarosa [18].

Regarding the importance of using the HiTAC technique in the process industries, in the present research the use of a theoretical

†To whom correspondence should be addressed.
E-mail: masoudrahimi@yahoo.com

(a) HRSG boiler (b) Real finned tube

Fig. 1. The HRSG boiler of the fajr petrochemical complex and a real finned tube.

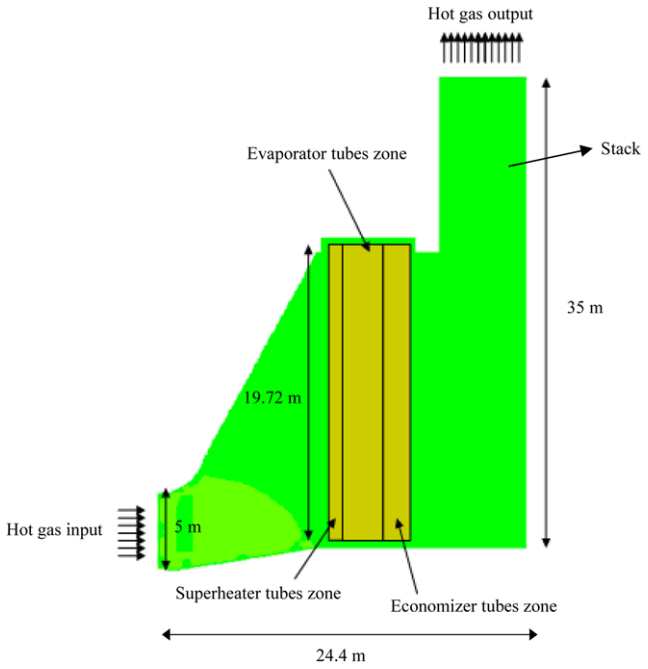

Fig. 2. The HRSG boiler dimensions and the location of three tube batches in the boiler.

HiTAC burner in the HRSG boiler of Fajr petrochemical Complex of Iran has been investigated. The main aim of this work is to illustrate the possibility of using HiTAC technology in a real boiler to increase its steam generating load. The employed burner can be useful to generate steam with a higher temperature without generating high temperature zones. The best nozzle location as well as the optimum input mass flow rate of the natural gas has been found by using CFD modeling.

THE HRSG BOILER DESCRIPTION

Fig. 1 shows the HRSG boiler as well as a real, finned superheater tube. The HRSG boiler is installed after a turbine's outlet hot gas and generates 182 ton/hr of steam with a pressure of 42 atm. The HRSG boiler has a height of 21.9 m, a length of 24.4 m. The hot gas enters the boiler through a 5 m square duct. The mass flow rate of inlet hot gas into the HRSG boiler is 428 kg/s and its temperature is 527 °C with a 15 percent air in excess.

The HRSG boiler includes three banks of tubes including economizer, evaporator and superheater. The superheater tube bank has 32 rows, of which every row covers 38 vertical finned tubes. Every tube has a height of 19.7 m, an inner diameter of 33.3 mm and a thickness 2.4 mm. Each tube is covered with 140,000 rectangular fins. Each fin has a height of 18 mm and a thickness of 1.1 mm. Fig. 2 shows the HRSG boiler dimensions and the location of these three tube types in the boiler.

The superheater tubes are arranged in 4 rows each with 38 tubes which are connected to two header boxes placed at the bottom and top of the boiler. The inlet saturated steam mass flow rate into each superheater tube is 0.333 kg/s with a temperature of 253 °C. The steam exits from these tubes at 427 °C with a pressure of 42 atm.

CFD MODELING

In the present research the commercial CFD package, FLUENT6.2 [19] was used to model the described HRSG boiler. A three-dimensional CFD simulation was carried out in order to model the combustion process as well as fluid and heat transfer to the boiler's superheater tubes. Regarding the large number of installed fins on each tube, the CFD modeling of the system was impossible. Therefore, the modeling was carried out for plain tube and then the predicted results were corrected for the finned one using the fin effectiveness coefficient. This parameter has been defined as follows.

$$\text{Fin effectivness coefficient} = \frac{\text{heat transfer rate with fin}}{\text{heat transfer rate without fin}} \quad (1)$$

The predicted mean convection heat transfer coefficients for plain and finned surfaces were used to calculate this parameter.

1. The Governing Equations

The CFD modeling involves with the numerical solution of the conservation equations. In the most of the research, the simulation solution of continuity and the Reynolds Averaged Navier Stocks equations was carried out by CFD codes. In the case of turbulent flow the random nature of flow precludes computations based on a complete description of the motion of all the fluid particles. In general, it is most attractive to characterize turbulent flow by the mean values of flow properties and the statistical properties of their fluctuations. In this study, 3-D Reynolds Averaged Navier Stokes equations together with RNG k–ε turbulence model [20] are solved with commercial CFD software, Fluent 6.2. The RNG turbulence model was derived by using a rigorous statistical technique (called renormalization group theory) and was used to predict better results for

round jets. The turbulence model is a semi-experimental model based on model transport equations for turbulence kinetic energy (k) and its dissipation (ε), which has been obtained from the following transport equations:

$$\frac{\partial(\rho k)}{\partial t}+\mathrm{div}(\rho k U)=\mathrm{div}\left[\frac{\mu_{eff}}{\sigma_k}\mathrm{grad}\ k\right]+G-\rho\varepsilon \quad (2)$$

$$\frac{\partial(\rho\varepsilon)}{\partial t}+\mathrm{div}(\rho\varepsilon U)=\mathrm{div}\left[\frac{\mu_{eff}}{\sigma_\varepsilon}\mathrm{grad}\ \varepsilon\right]+C_{1\varepsilon}\frac{\varepsilon}{k}2\mu_{eff}E_{ij}\cdot E_{ij}-C_{2\varepsilon}\rho\frac{\varepsilon^2}{k} \quad (3)$$

where

$$\mu_{eff}=\mu+\mu_T,\quad \mu_T=\rho C_\mu\frac{k^2}{\varepsilon} \quad (4)$$

where t is time, ρ is the density, U is the mean velocity, μ is the laminar viscosity, μ_T is the turbulent viscosity, μ_{eff} is the effective viscosity, G is the dissipation function, E_{ij} is the linear deformation rate, σ_k and σ_ε are the turbulence Prandtl numbers and $C_{1\varepsilon}$, $C_{2\varepsilon}$ and C_μ are model constants as follows.

$C_{1\varepsilon}$=1.42 $C_{2\varepsilon}$=1.68 C_μ=0.0845 σ_k=1.00 σ_ε=1.30

The proper simulation of non-premixed turbulent combustion processes requires an effective scheme for simultaneously modeling both the mixing and the reactions of relevant chemical species. As a starting point, in keeping with the approach used for the mass, momentum, and energy equations, a partial differential conservation equation can be written for each of the chemical species as follows:

$$\frac{\partial(\rho m_i)}{\partial t}+\frac{\partial(\rho u_i m_i)}{\partial x_i}=\frac{\partial}{\partial x_i}\left(\frac{\mu_e\partial m_i}{\sigma_m\partial x_i}\right)+R_i+S_i \quad (5)$$

where m_i is the mass fraction of the ith chemical species, σ_m is the ratio of effective diffusion coefficient for the ith species and the turbulent momentum diffusivity, μ_e is the dynamic eddy viscosity, R_i is the mass rate of creation or depletion by chemical reaction and S_i represents other sources of species creation. The chemical production or depletion term, R_i, can be determined (on a mass/volume basis) as follows.

$$R_i=(v_i''-v_i')M_i k\prod_l C_l^{v_l} \quad (6)$$

where v_i'' and v_i' are the stoichiometric coefficients for the ith species as a product and a reactant, respectively, M_i is the molecular weight of the ith species, k is the specific reaction rate constant, C_l is the molar concentration of the lth reactant species and v_l is the stoichiometric coefficient of the lth reactant species. The reaction rate constant, k, is expressed by the modified Arrhenius equation.

$$k=AT^\alpha\exp\left(\frac{-E}{RT}\right) \quad (7)$$

where α, A and E are reaction rate parameters, R is the ideal gas constant and T is the temperature. In this work, for turbulent reacting flows, the eddy dissipation model [21] was used. The eddy dissipation model is suitable for a wide range of applications including premixed, partially premixed, and non-premixed turbulent combustion.

To predict the radiative heat transfer in the boiler, the radiative transfer equation (RTE) for an absorbing, emitting and scattering medium was solved. In the present research, the Rosseland model [22] was used for solving the RTE. This model is valid when the medium is optically thick ($(a+\sigma_l)L>1$), where a is the absorption coefficient, σ_l is the scattering coefficient and L is the length of the boiler. In the present study, the optical thickness is about 2 so the Rosseland model is suitable for this case. The WSGGM (weighted sum of gray gas) model [23] is used to calculate the total emissivity as a function of gas composition and temperature.

2. Boundary Conditions

The operating conditions at maximum steam capacity of 182,000 kg/hr are summarized as follows:

- The inlet hot gases into the HRSG boiler with 15% air in excess (mass flow rate: 428 kg/s; temperature: 527 °C).
- The outlet of the HRSG boiler stack (pressure outlet: the atmospheric pressure; temperature: 27 °C).
- The inlet saturated steam into the superheater tube (mass flow rate: 0.333 kg/s; pressure: 42 atm; temperature: 253 °C).
- The outlet saturated steam (pressure outlet: 42 atm).

3. Solution Method

The governing equations of the system are solved by finite volume method employing the semi implicit method for pressure linked equations (SIMPLE) algorithm, the standard pressure and the second order upwind discretization scheme for momentum, turbulent kinetic energy and dissipation energy. The set of governing differential equations together with the boundary conditions are to be solved numerically by an iterative, line-by-line procedure. The convergence criterion was based on the residual value of the calculated variables, namely continuity, velocity components and energy. In the present calculations, a convergence criterion of 10^{-5} was chosen for all calculated parameters. The total number of iterations was 15467 to reach converged values.

4. Mesh Layout

The HRSG boiler was meshed into almost 1,158,642 unstructured tetrahedral control volumes. The regions close to the super-

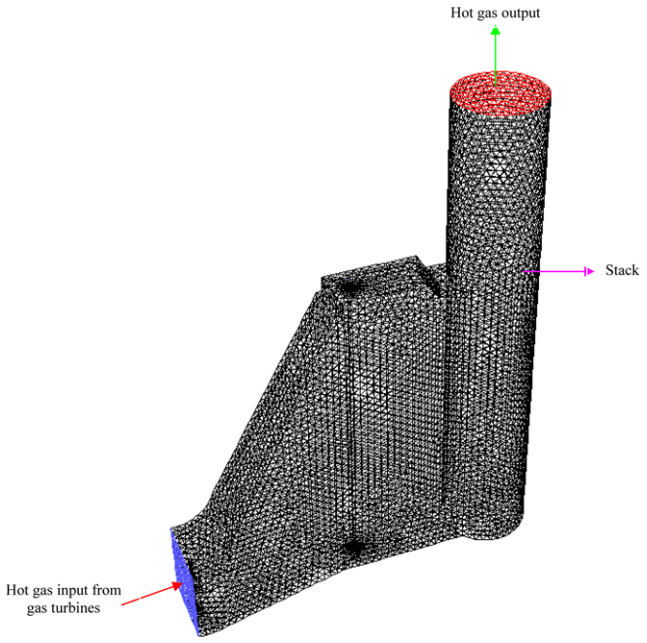

Fig. 3. The modeled HRSG boiler.

Table 1. The predicted steam temperatures (°C) at various grid sizes

Grid 4 (1428632 meshes)	Grid 3 (1158642 meshes)	Grid 2 (946234 meshes)	Grid 1 (757136 meshes)	Tube length (m)
253	253	253	253	0
267.73	267.87	265.11	261.47	2
281.23	281.75	282.48	278.22	4
295.91	296.12	298.65	290.31	6
311.05	310.81	312.36	315.27	8
324.67	324.87	327.13	318.83	10
339.11	338.43	335.21	331.55	12
352.50	352.67	353.75	348.32	14
366.32	366.43	367.96	362.38	16
379.81	379.87	377.16	372.75	18
397.46	397.37	394.31	390.12	20

heater tube and natural gas nozzle were divided into smaller meshes for more precise prediction. Fig. 3 shows the modeled HRSG boiler and a view from its meshed layout. To ensure the solution independency from the grid size, the geometry was meshed using four different grid sizes, and the temperature of the steam at various lengths of the tube was predicted. In Table 1 the predicted steam temperatures at various examined grid sizes are reported. The results show that the predicted temperatures using Grid3 and 4 setups are quite close together. In the other words, the prediction dependency for more number of control volumes than Grid3 is negligible. Therefore, due to its less required computation time, Grid3 setup was chosen for modeling in the present study.

CFD VALIDATION

To measure the rate of heat transfer in superheater tubes, a plain superheater tube in HRSG boiler was modeled using the previous mentioned operating conditions. The fin effectiveness coefficient of 3.125 was found from Eq. (1) and used in order to correct the obtained temperatures.

In the model, the inlet steam temperature of the superheater tube was chosen to be 253 °C, which is the same as the real condition. In this condition, the predicted outlet steam temperature for the plain tube was 299 °C, which shows a 45 °C increase across the tube. Using the obtained fin effectiveness coefficient, an outlet steam temperature of 397 °C was obtained for the finned tube. From performance test results done in the Fajr Petrochemical Complex, an outlet steam temperature of 427 °C was obtained, which means the error between the modeling and the test results is 7.5 percent. The lower predicted temperature can be related to single tube modeling conducted in this study, which ignores the effect of passing of the hot gas through the bundle of tubes. In addition, modeling of a plain tube and correcting the results with the fin effectiveness coefficient can be another reason for this difference.

RESULTS AND DISCUSSION

In the present research, the HiTAC technique is used to increase the HRSG boiler steam temperature. A natural gas nozzle with a diameter of 10 cm is placed inside the boiler inlet hot gas stream and we have attempted to find the proper nozzle position and gas flow rate. The inlet natural gas temperature is defined to be 27 °C.

1. The Natural Gas Nozzle Position Selection

To find the proper position for the natural gas nozzle inside the boiler, three different positions have been examined using CFD modeling. In all layouts the mass flow rate of natural gas is defined to be 1 kg/s. The studied nozzle positions are as follows:

- Position 1: The nozzle is placed in the upper side of the HRSG inlet duct at a height of 12 m from the boiler bottom and a distance of 4.7 m in front of the hot gas entrance.
- Position 2: The nozzle is located at 5 m from the boiler entrance and a height of 2.5 m from the boiler bottom.
- Position 3: The nozzle is placed 0.5 m from the boiler entrance and a height of 2.5 m from the boiler bottom.

Fig. 4 shows the nozzle positions as well as the temperature profiles in each position. As can be seen in Fig. 4(a), related to position 1, combustion has taken place in a region with a low flow rate of the carrier gas. This caused an abnormal increase in temperature in the area close to the boiler's wall. On the other hand, by comparing the temperature profile of positions 2 and 3, the results illustrate that a high temperature region covers the whole tube for position 3 (Fig. 4(c)). However, this hot region could not cover the whole tube for position 2 (Fig. 4(b)). Therefore, more efficient temperature distribution has been found for position 3.

More quantitatively, a comparison between the temperature profile inside the superheater tube for positions 2 and 3 is shown in Fig. 5. The figure reveals that the outlet steam temperature from the superheater tube is 486 °C and 495 °C as the nozzle placed in positions 2 and 3, respectively. This confirms that the rate of heat transfer to the superheater tube for position 3 nozzle layout is more efficient than that of position 2.

2. The Natural Gas Mass Flow Rate Determination

In the next step of the present modeling, after identifying the proper place for the nozzle, the optimum mass flow rate of the natural gas was investigated in order to increase the boiler efficiency. For this purpose, the mass flow rate of natural gas diverted to the nozzle was varied from 0 to 2 kg/s. Fig. 6 shows the steam temperature profile inside the tube at various natural gas mass flow rates. As expected, due to more heat of combustion at higher fuel flow rates, the temperature of the steam in the superheater tube increased at higher natural gas flow rates. However, Fig. 7 illustrates that an increase of the natural gas mass flow rate causes a higher established tube wall temperature. Since the maximum allowable temperature of the tube is about 600 °C, the mass flow rate for the HiTAC nozzle should not be more than 0.5 kg/s.

3. Advantage of Using HiTAC Technique

In Fig. 8 the temperature profiles in the superheater tube for HRSG boiler equipped with HiTAC nozzle are compared with a similar one without a nozzle. The nozzle was installed in the above described proper place (position 3) and natural gas with a mass flow rate of 0.5 kg/s was diverted into the nozzle. As shown in the figure, the predicted outlet steam temperatures are 397 °C and 451 °C for the enhanced and present systems, respectively. In the other words, according to the inlet steam temperature by using a HiTAC burner the rate of heat transfer to a superheater tube can be increased up to 37%.

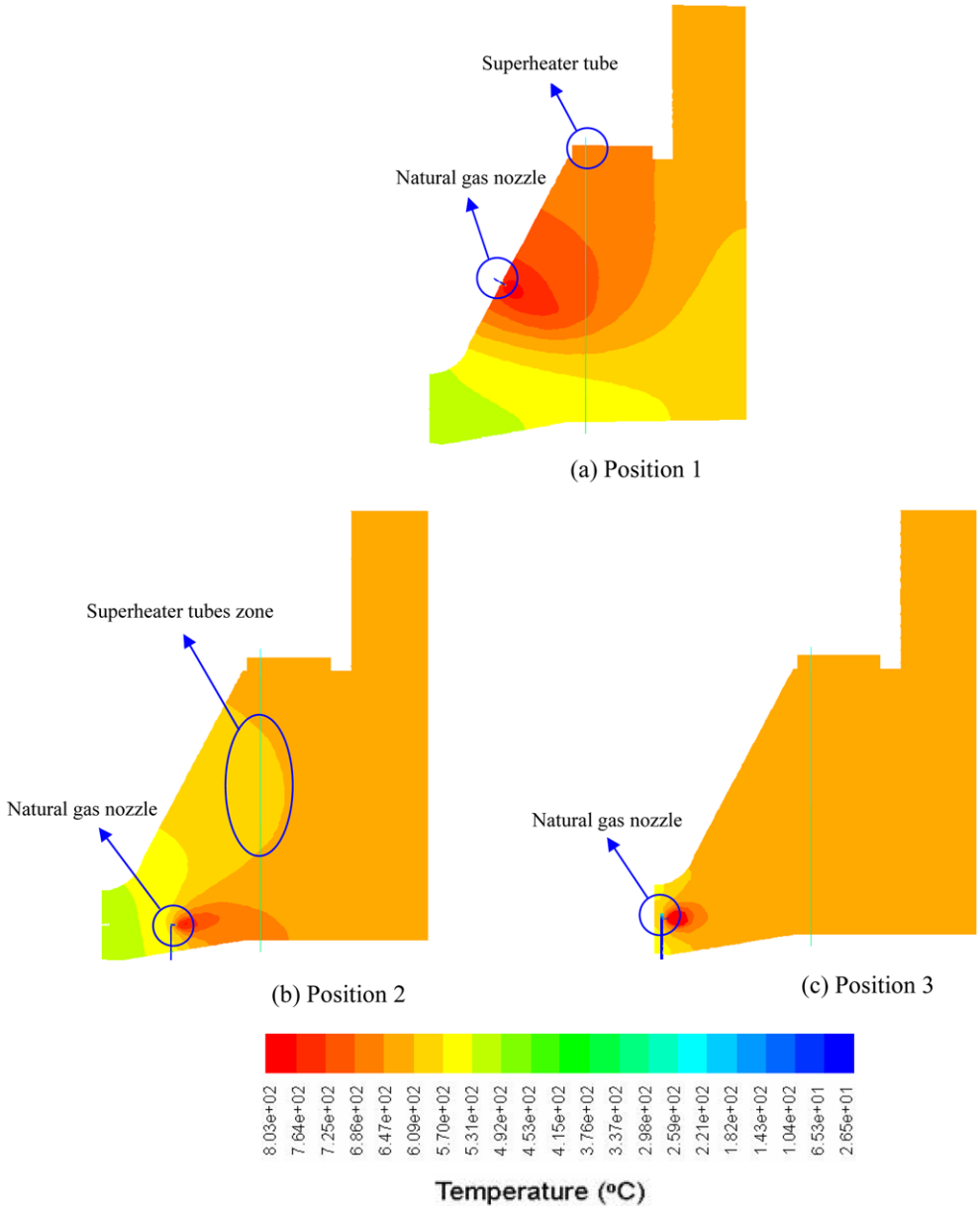

Fig. 4. The temperature profiles of three different positions for natural gas nozzle.

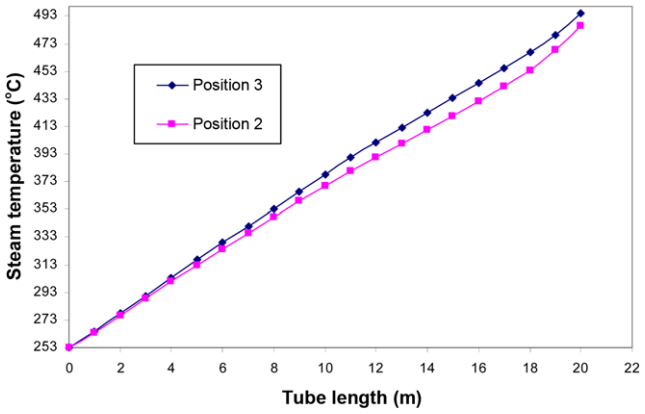

Fig. 5. The steam temperature inside the superheater tube in the positions 2 and 3.

CONCLUSION

The present study illustrates how it is possible to use the HiTAC technique in an HRSG boiler. In this work it has been theoretically tried to use the high temperature waste gas to establish the new developed combustion technique, HiTAC. The results show that the fuel nozzle position as well as amount of fuel can have significant effects on the obtained outlet steam temperature. These have been found by using CFD modeling without the need for any expensive experimental tests. In the CFD modeling, complete modeling of tube was impossible due to the large number of installed fins on the real tubes, which are 140,000 per tube. Therefore, a fin effectiveness coefficient has been proposed to find the heat transfer rate to the finned tube from modeling predictions of the plain one. The results show that by adding a natural gas nozzle to the studied boiler

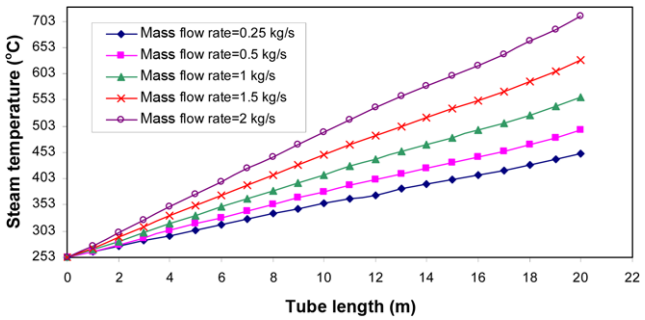

Fig. 6. The steam temperature inside the tube with different mass flow rates of the natural gas.

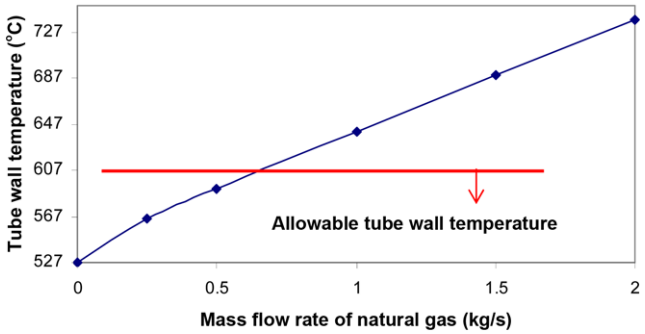

Fig. 7. The tube wall temperature at various mass flow rates of the natural gas.

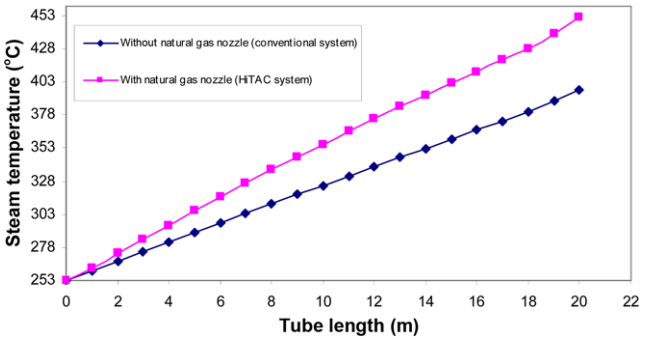

Fig. 8. The steam temperature along the superheater tube with and without HiTAC burner.

it is feasible to increase outlet steam temperature up to 37%. This study reveals one application of the HiTAC technique in a real industrial boiler and the possibility of using this system in any previously designed HRSG boiler.

ACKNOWLEDGEMENT

The authors wish to express their thanks to the Iranian Petrochemical Research and Technology Company for the financial support of this work. Also, Mr. Dokouhaki's help during this research is greatly appreciated.

NOMENCLATURE

a : absorption coefficient
$C_{1\varepsilon}$, $C_{2\varepsilon}$, C_{μ} : constants of the model
C_l : molar concentration of the *l*th reactant species [Kgmol·m^{-3}]
E_{ij} : linear deformation rate
G : dissipation function [Pa·s^{-1}]
k : turbulent kinetic energy [J·Kg^{-1}]
m_l : mass fraction
M_i : molecular weight of the *i*th species [Kg·Kgmol^{-1}]
R_i : mass rate of chemical reaction [Kg·m^{-3}·s^{-1}]
t : time [s]
T : temperature [K]
U : mean velocity [m·s^{-1}]

Greek Symbols

ε : turbulence dissipation [m·s^{-1}]
μ, μ_t, μ_{eff} : Laminar, turbulent and effective viscosities [Pa·s]
v_i', v_i'' : stoichiometry coefficients for the *i*th species
ρ : density [Kg·m^{-3}]
σ_k, σ_ε : turbulent Prandtl numbers for k–ε
σ_l : scattering coefficient
σ_m : ratio of effective diffusion coefficient

REFERENCES

1. R. Tanaka and T. Hasegawa, *Innovative technology to change flame characteristics with highly preheated air combustion*, Proceedings of Japanese Flame Days, Osaka, 129 (1997).
2. L. Kong, Y. Ding, Y. Zhang, L. Yuan and Z. Wu, *Korean J. Chem. Eng.*, **26**, 534 (2009).
3. S. R. Wu, W. C. Chang and J. Chiao, *Fuel*, **86**, 820 (2007).
4. D. H. Chung, J. B. Yang, D. S. Noh and W. B. Kim, *Korean J. Chem. Eng.*, **16**, 489 (1999).
5. E. Benini, S. Pandolfo and S. Zoppellari, *Appl. Therm. Eng.*, **29**, 3506 (2009).
6. K. Kitagawa, N. Konishi, N. Arai and A. K. Gupta, *J. Gas. Turb. Power*, **125**, 326 (2003).
7. A. K. Gupta and Z. Li, *J. Energy Res.*, **5**, 247 (1997).
8. F. C. Christo and B. B. Dally, *Combust. Flame*, **142**, 117 (2005).
9. S. Lille, W. Blasiak and M. Jewartowski, *Energy*, **30**, 373 (2005).
10. S. H. Kim, K. Y. Huh and B. Dally, *Proc. Combust. Inst.*, **30**, 751 (2005).
11. M. Rahimi, A. Khoshhal and S. M. Shariati, *Appl. Therm. Eng.*, **26**, 2192 (2006).
12. A. Khoshhal, M. Rahimi and A. A. Alsairafi, *Int. Commun. Heat Mass Trans.*, **36**, 750 (2009).
13. H. K. Seo, D. Shin, J. H. Chung, B. Kim, S. M. Park and H. C. Lim, *Korean J. Chem. Eng.*, **26**, 72 (2009).
14. H. Liu, N. Xin, Q. Cao, L. Sha, D. Sun and S. Wu, *Korean J. Chem. Eng.*, **26**, 1137 (2009).
15. S. Orsino, R. Weber and U. Bollettini, *Combust. Sci. Technol.*, **170**, 1 (2001).
16. K. Kawai, K. Yoshikawa, H. Kobayashi, J. S. Tsai, M. Matsuo and H. Katsushima, *Energy Convers. Manage.*, **43**, 1563 (2002).
17. K. A. Khazaei, A. A. Hamidi and M. Rahimi, *Chin. J. Chem. Eng.*, **17**, 711 (2009).
18. A. Franco and C. Casarosa, *Appl. Therm. Eng.*, **22**, 1501 (2002).
19. Fluent Inc., Fluent 6.2 User's Guide (2005).
20. H. K. Versteeg and W. Malalasekera *An introduction to computa-*

tional fluid dynamics; the finite volume method, Longman Scientific and Technical (1995).
21. B. F. Magnussen and B. H. Hjertager, *On mathematical models of turbulent combustion with special emphasis on soot formation and combustion*, 16th Symposium on combustion, The Combustion Institute (1976).
22. R. Siegel and J. R. Howell, *Thermal radiation heat transfer*, 3rd Ed. Washington, Hemisphere Publishing Corporation (1992).
23. E. Chui and G. Raithby, *Numeric. Heat Transfer, Part B*, **23**, 269 (1993).